

Electronic Supplementary Information for

**Boron-doped silver nanosponges with enhanced performance towards
electrocatalytic nitrogen to ammonia**

Yinghao Li, Hongjie Yu, Ziqiang Wang,* Songliang Liu, You Xu, Xiaonian Li, Liang Wang,*

Hongjing Wang*

State Key Laboratory Breeding Base of Green-Chemical Synthesis Technology, College of
Chemical Engineering, Zhejiang University of Technology, Hangzhou 310014, P. R. China.

E-mails: zqwang@zjut.edu.cn; wangliang@zjut.edu.cn; hjw@zjut.edu.cn

1. Materials synthesis

1.1 Materials and Chemicals. Ammonium chloride (NH_4Cl , 99.999%) and sodium nitroferricyanide dihydrate ($\text{C}_5\text{FeN}_6\text{Na}_2\text{O}\cdot 2\text{H}_2\text{O}$, $\geq 99.0\%$) were purchased from MACKLIN. Silver nitrate (AgNO_3 , 99.8%), salicylic acid ($\text{C}_7\text{H}_6\text{O}_3$, 99.5%), sodium borohydride (NaBH_4 , 96%), para-(dimethylamino) benzaldehyde ($\text{C}_9\text{H}_{11}\text{NO}$, 99%), *N,N*-dimethylformamide (DMF, 99.5%), sodium hypochlorite solution (NaClO , available chlorine 6.0–14.0%), concentrated hydrochloric acid (HCl , 37 wt%), ethanol ($\text{C}_2\text{H}_5\text{OH}$, $\geq 99.8\%$), and hydrazine monohydrate ($\text{N}_2\text{H}_4\cdot\text{H}_2\text{O}$, $\geq 99\%$) were purchased from Aladdin. Nafion solution (5 wt%) was ordered from the Sigma-Aldrich. Carbon paper and Nafion 117 membranes were received from Shanghai Hesen Electric Co., Ltd.

1.2 Synthesis of B-Ag NSs. In a typical preparation of B-Ag NSs, 17 mg of AgNO_3 was dissolved in 1 mL of DMF under ultrasonication. Then 5 mL of DMF containing 18.9 mg of NaBH_4 was quickly injected into above solution, which was maintained in an ice bath for 2 h with vigorous stirring. Finally, the final product was collected by centrifugation and washed several times with ethanol and water.

2. Characterization

Scanning electron microscopy (SEM) images were obtained by a JSM-2010 scanning electron microscope. Transmission electron microscopy (TEM) and elemental analysis mapping were performed on a JEOL JEM-2100 equipped with an energy dispersive X-ray (EDX) spectroscopy. X-ray photoelectron spectroscopy (XPS) measurements were carried out using an ESCALAB MK II spectrometer. The X-ray diffraction (XRD) patterns were collected on an X-ray diffractometer (Shimadzu, XRD-6000) with $\text{Cu K}\alpha$ radiation. The compositions of the catalysts were measured by inductively coupled plasma mass spectrometry (ICP-MS) (Elan DRC-e instrument).

3. Electrochemical measurements

All electrochemical measurements were performed in a two-compartment cell separated by a Nafion 117 membrane at ambient temperature. Three-electrode system was employed to estimate electrochemical performance by a CHI 660E apparatus, where modified carbon cloth, saturated

Ag/AgCl electrode and carbon rod were used as the working electrode, reference electrode and counter electrodes, respectively. For preparation of the working electrode, 5 mg of catalyst was mixed with 50 μL of Nafion solution (5 wt%), 300 μL of ultrapure water and 650 μL of ethanol with sonication for 2 h. Then 20 μL of electrocatalyst ink was loaded onto carbon paper ($0.5 \times 0.5 \text{ cm}^2$) and dried under room temperature. Before N_2 reduction experiments, the electrolyte (0.1 M HCl) was purged with N_2 for 30 min. Linear sweep voltammetry (LSV) curves of catalysts were conducted in N_2 - or Ar-saturated 0.1 M HCl solution. The chronoamperometry test was performed at different potentials in the N_2 -saturated 0.1 M HCl solution with continual bubble of N_2 . Potentials were recorded on the reversible hydrogen electrode, and current densities were normalized to geometric area of carbon cloth.

4. Production Quantification

The concentration of produced NH_3 was determined by the indophenol blue method.¹ In detail, 2 mL of electrolyte after electrolysis was mixed with 2 mL of 1.0 M NaOH solution containing $\text{C}_7\text{H}_6\text{O}_3$ (5 wt%) and $\text{C}_6\text{H}_5\text{Na}_3\text{O}_7$ (5 wt%), 1 mL of 0.05 M NaClO solution, and 0.2 mL of $\text{C}_5\text{FeN}_6\text{Na}_2\text{O}$ solution (1 wt%). After standing at 25 $^\circ\text{C}$ for 2 h in the dark, the absorption spectrum was detected by an ultraviolet-visible (UV-vis) spectrophotometer. The known concentration NH_4^+ solutions were used to calibrate the concentration-absorbance standard curve. On the other hand, the probable by-product hydrazine was estimated by the method of Watt and Chrisp.² Typically, the mixture solution containing 5.99 g of $\text{C}_9\text{H}_{11}\text{NO}$, 300 mL of ethanol and 30 mL of HNO_3 was used as a color reagent. Then, 5 mL of electrolyte after electrolysis was added into 5 mL of color reagent. After standing for 10 min, the UV-vis absorption spectra were measured. The known concentration hydrazine monohydrate solutions were used to calibrate the concentration-absorbance standard curve. The rate of formation of NH_3 (v_{NH_3}) was calculated according to the following equation:

$$v_{\text{NH}_3} = (c_{\text{NH}_3} \times V) / t \times m \quad (1)$$

The FE was calculated based on the following equation:

$$\text{FE} = 3F \times c_{\text{NH}_3} \times V / (17 \times Q) \quad (2)$$

where c_{NH_3} is the concentration of NH_3 in the electrolyte; V is the volume of electrolyte; t is the electrolysis time; m is the mass of catalysts; F is the Faraday constant; and Q is the total quantity of applied electricity.

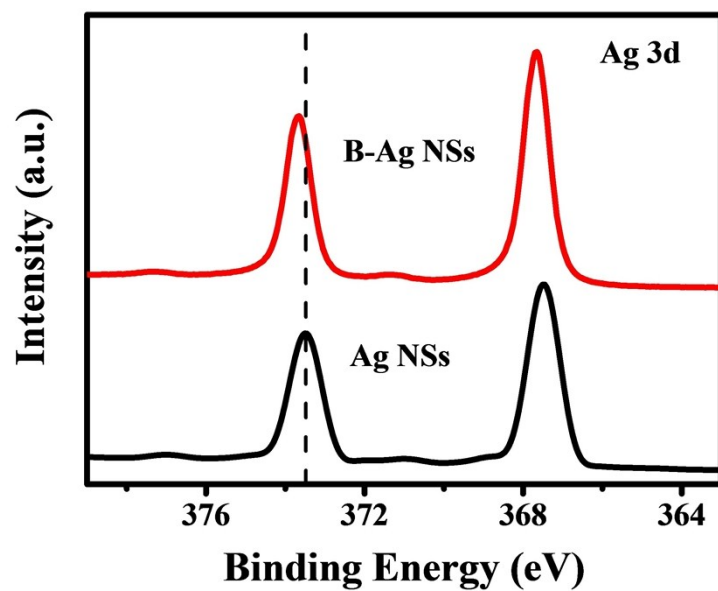


Fig. S1 XPS Ag 3d spectra of the B-Ag NSs and Ag NSs.

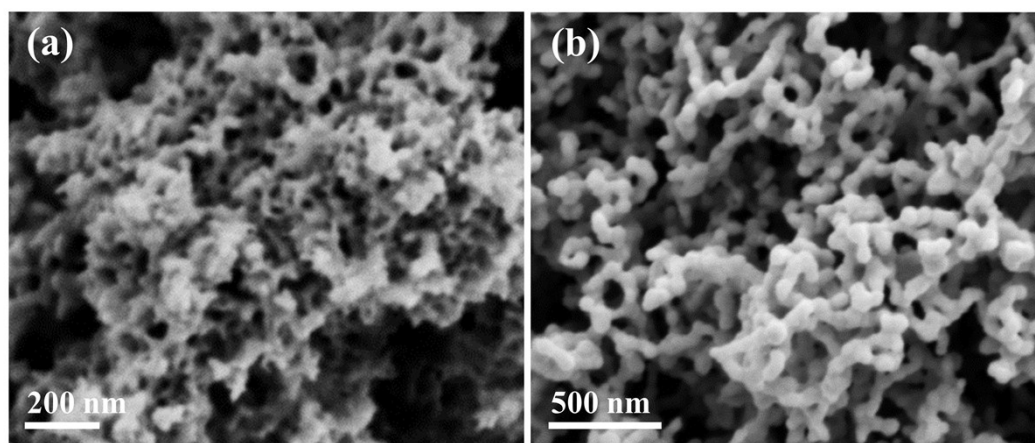


Fig. S2 SEM images of the samples prepared with different solvents: (a) H₂O and (b) DMF.

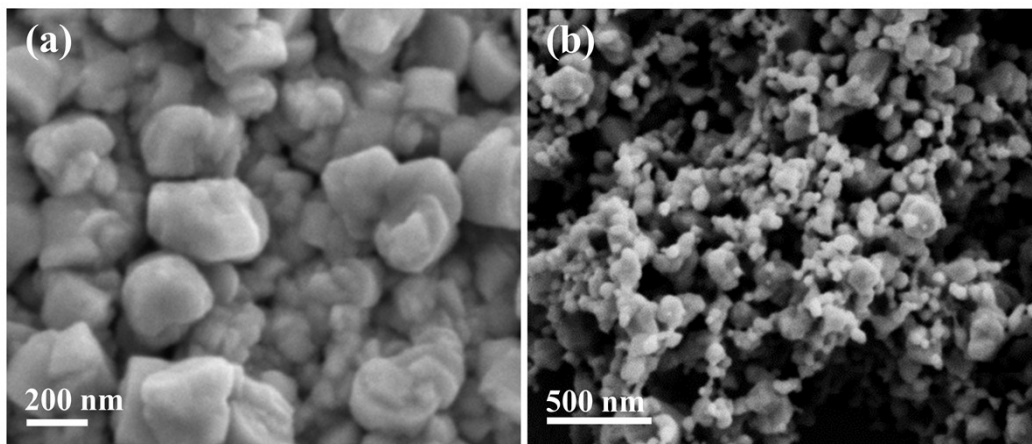


Fig. S3 SEM images of the samples prepared with different concentrations of NaBH_4 : (a) 20 mM and (b) 0.5 M.

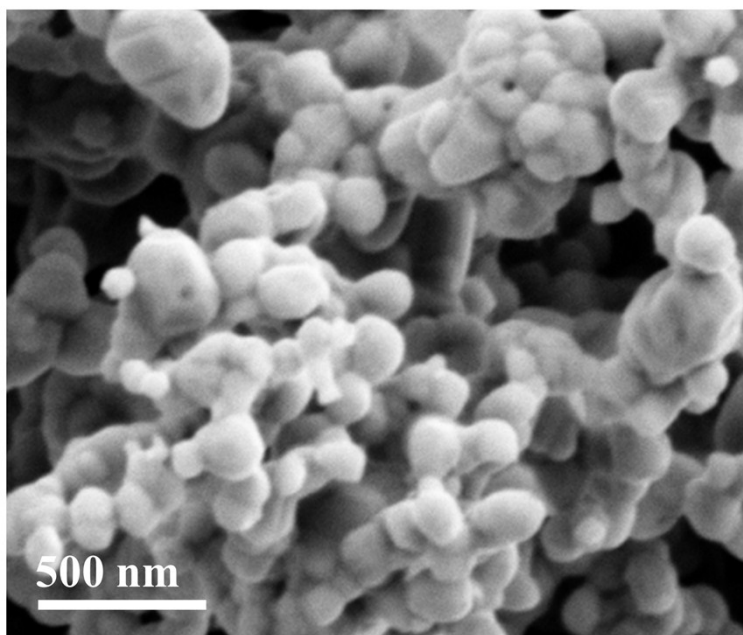


Fig. S4 SEM image of the sample prepared at room temperature.

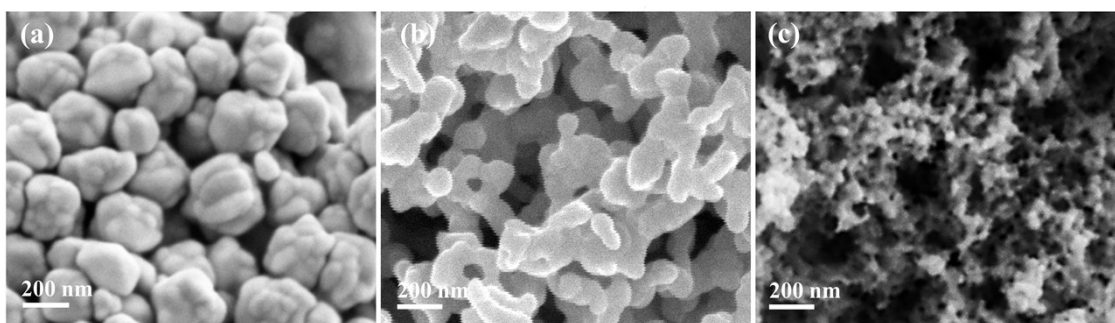


Fig. S5 SEM images of the samples prepared with different amounts of reducing agent and metallic precursor: (a) NaBH₄ (1 mL, 0.1 M), AgNO₃ (1 mL, 0.1 M); (b) NaBH₄ (1 mL, 0.1 M), AgNO₃ (3 mL, 0.1 M); and (c) NaBH₄ (1 mL, 0.1 M), AgNO₃ (10 mL, 0.1 M).

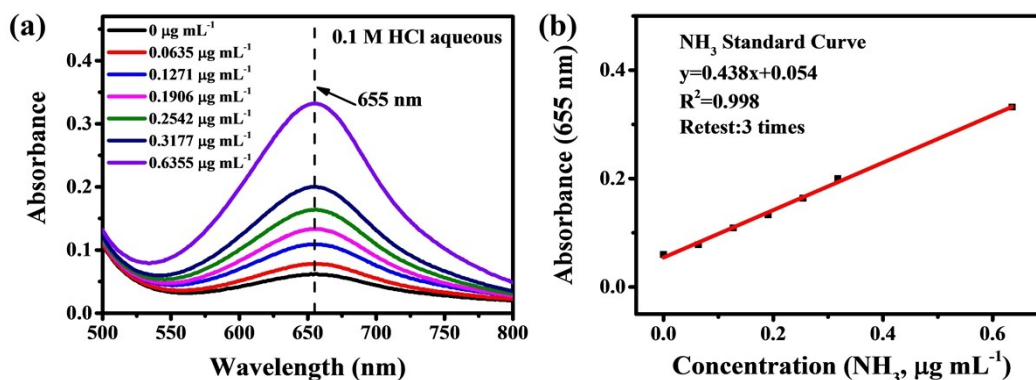


Fig. S6 Absolute calibration of the indophenol blue method using ammonium chloride solutions of known concentrations as standards. (a) UV-vis absorption spectra of indophenol assays with NH₄⁺ ions after incubation for 2 h at room temperature. (b) Calibration curve used for estimation of NH₃ by NH₄⁺ concentrations. The absorbance at 655 nm was measured by UV-vis spectrophotometer, and the fitting curve shows good linear relation of absorbance with NH₃ concentrations.

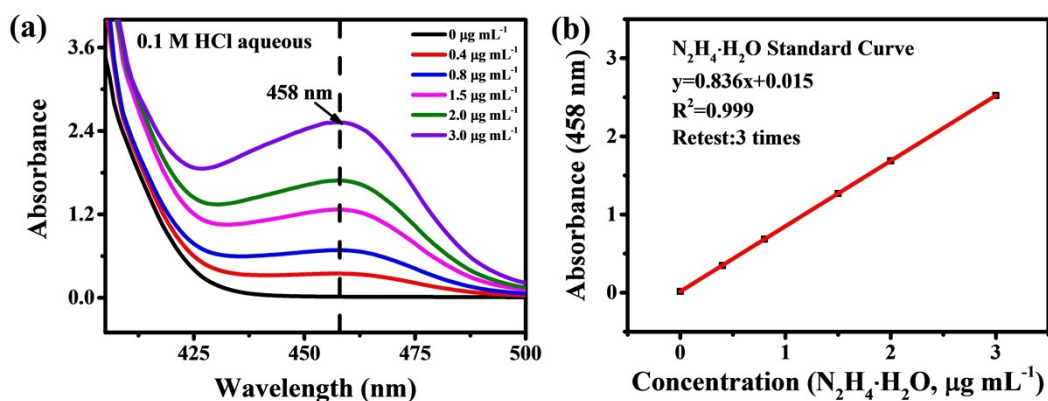


Fig. S7 Absolute calibration of the Watt and Chrisp (para-dimethylaminobenzaldehyde) method for the estimating of $\text{N}_2\text{H}_4 \cdot \text{H}_2\text{O}$ concentration using $\text{N}_2\text{H}_4 \cdot \text{H}_2\text{O}$ solutions with known concentration as standards. (a) UV-Vis curves of various $\text{N}_2\text{H}_4 \cdot \text{H}_2\text{O}$ concentration after incubated for 10 min at room temperature. (b) Calibration curve used for estimation of $\text{N}_2\text{H}_4 \cdot \text{H}_2\text{O}$ concentration. The absorbance at 458 nm was measured by UV-Vis spectrophotometer, and the fitting curve shows good linear relation of absorbance with $\text{N}_2\text{H}_4 \cdot \text{H}_2\text{O}$ concentration of three times independent calibration curves.

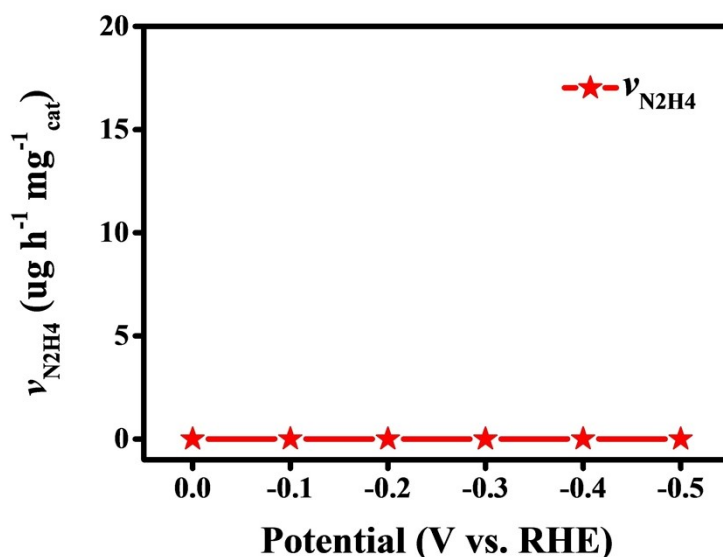


Fig. S8 Yield rate of N_2H_4 formation for the B-Ag NSs at selected potentials.

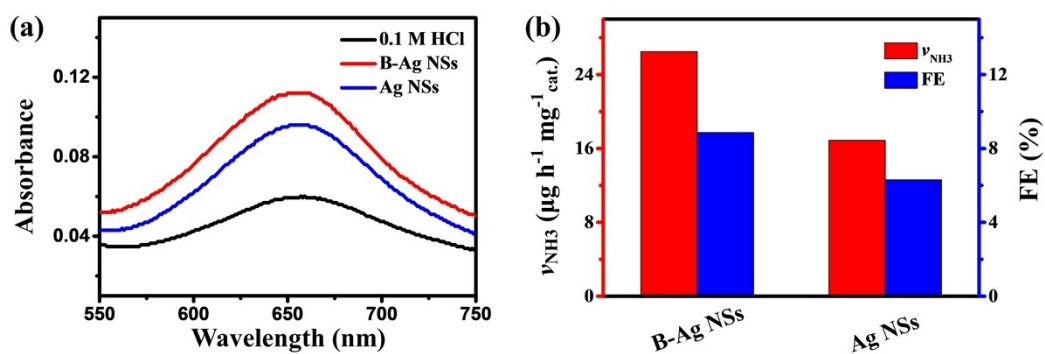


Fig. S9 (a) UV-vis absorption spectra of the electrolyte catalysed by the B-Ag NSs and Ag NSs. (b) Yield rate of NH₃ and corresponding FE of the B-Ag NSs and Ag NSs.

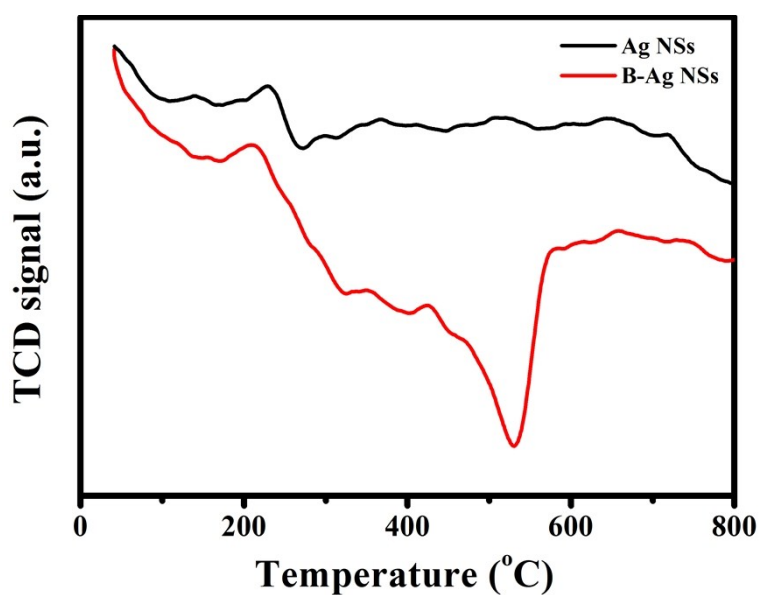


Fig. S10 N₂-TPD profiles of Ag NSs and B-Ag NSs.

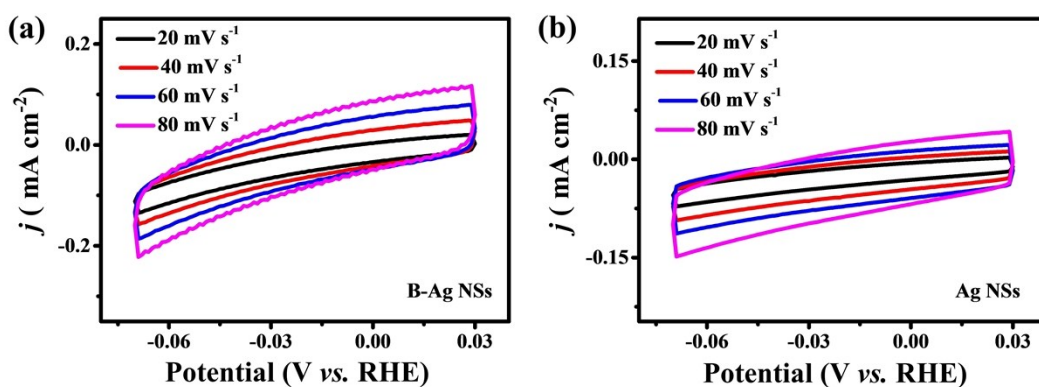


Fig. S11 cyclic voltammetry curves of the (a) B-Ag NSs and (b) Ag NSs at different scan rates in the potential range of -0.07 and 0.03 V.

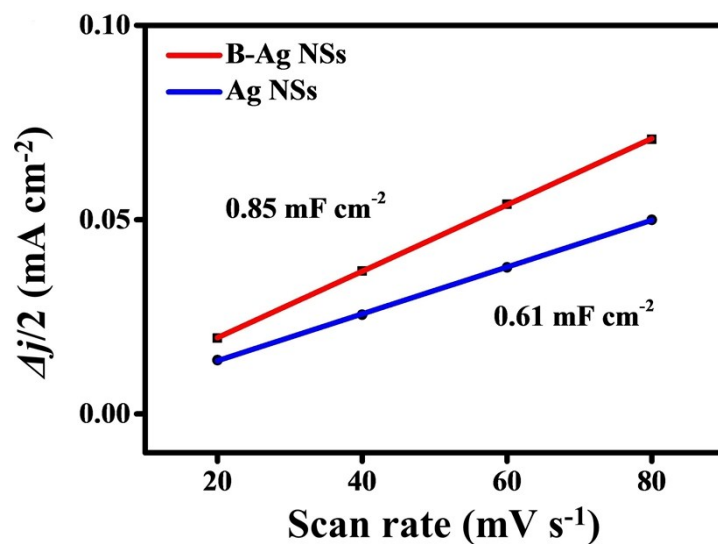


Fig. S12 Charging current density differences plotted against scan rates for the B-Ag NSs and Ag NSs.

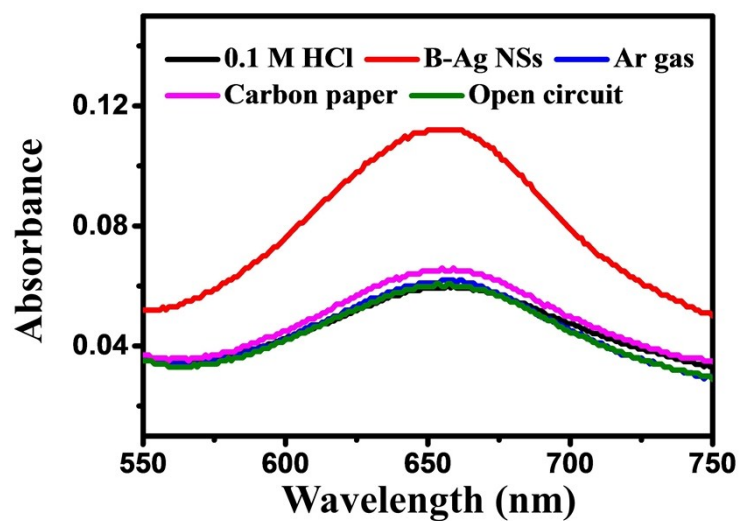


Fig. S13 UV-vis absorption spectra of HCl electrolytes stained with indophenol indicator after charging at -0.2 V for 2 h under various conditions.

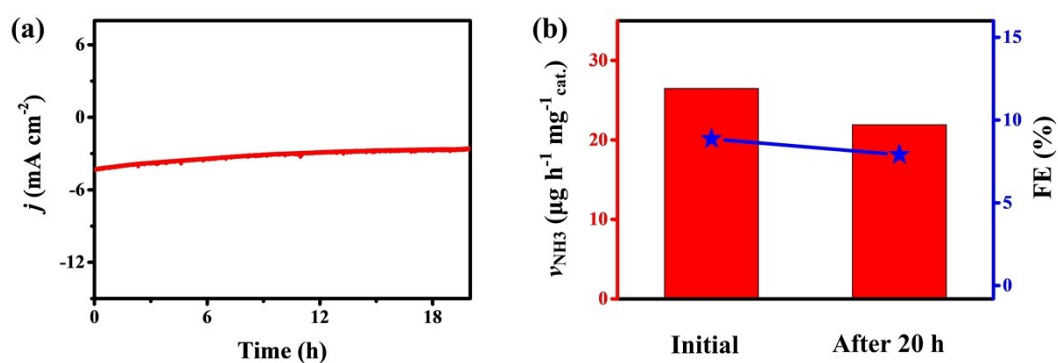


Fig. S14 (a) Chronoamperometry curve of the B-Ag NSs at the potential of -0.5 V for 20 h. (b) Yield rate of NH_3 and corresponding FE before and after the durability tests.

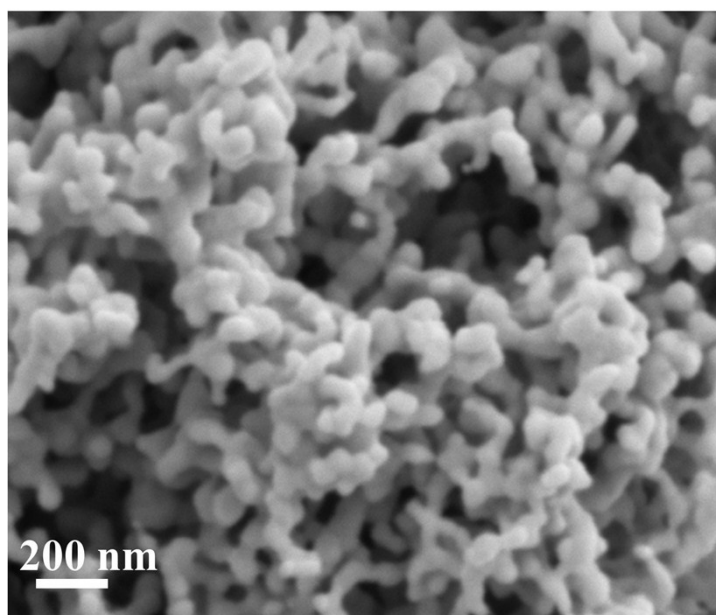


Fig. S15 SEM image of the B-Ag NSs after long-term stability measurement.

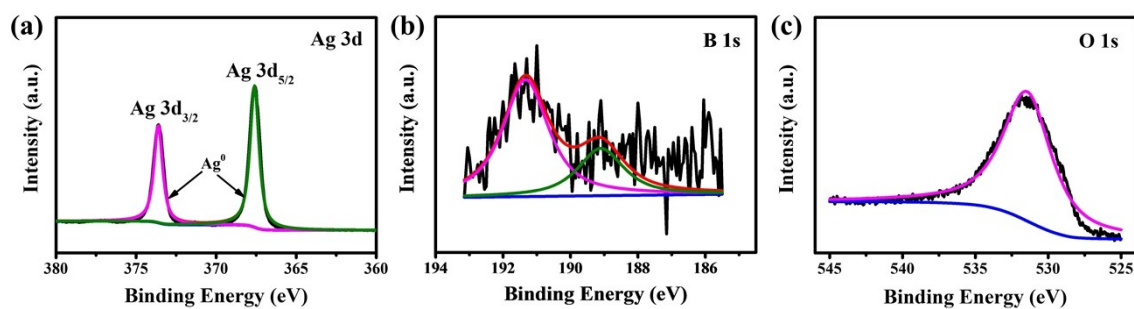


Fig. S16 XPS spectra of the Ag 3d, B 1s and O 1s for the B-Ag NSs after stability test.

Table S1. The comparisons of the NRR activity of the B-Ag NSs with the recently reported catalysts under ambient conditions.

Catalyst	Electrolyte	NH ₃ yield rate	FE(%)	Ref.
B-Ag NSs	0.1 M HCl	26.48 $\mu\text{g h}^{-1} \text{mg}^{-1}_{\text{cat}}$	8.86	This work
Au-TiO ₂ sub nanocluster	0.1 M HCl	21.4 $\mu\text{g h}^{-1} \text{mg}^{-1}_{\text{cat}}$	8.11	3
α -Au/CeO _x -rGO	0.1 M HCl	8.3 $\mu\text{g h}^{-1} \text{mg}^{-1}_{\text{cat}}$	10.1	4
VN nanosheet array	0.1 M HCl	5.6 $\mu\text{g h}^{-1} \text{mg}^{-1}_{\text{cat}}$	2.25	5
Pd/C	0.1 M HCl	$\sim 2.5 \mu\text{g h}^{-1} \text{mg}^{-1}_{\text{cat}}$	~ 1.0	6
Ag nanosheets	0.1 M HCl	2.83 $\mu\text{g h}^{-1} \text{mg}^{-1}_{\text{cat}}$	4.8	7
MoO ₃	0.1 M HCl	29.43 $\mu\text{g h}^{-1} \text{mg}^{-1}_{\text{cat}}$	1.9	8
PdRu BPNs	0.1 M HCl	25.92 $\mu\text{g h}^{-1} \text{mg}^{-1}_{\text{cat}}$	1.53	9
Au flower	0.1 M HCl	25.57 $\mu\text{g h}^{-1} \text{mg}^{-1}_{\text{cat}}$	6.05	10
N-Doped Porous Carbon	0.05 M H ₂ SO ₄	23.8 $\mu\text{g h}^{-1} \text{mg}^{-1}_{\text{cat}}$	1.42	11
Fe ₂ O ₃ -CNT	diluted KHCO ₃	0.22 $\mu\text{g h}^{-1} \text{cm}^{-2}$	0.15	12

References

1. D. Bao, Q. Zhang, F. L. Meng, H. X. Zhong, M. M. Shi, Y. Zhang, J. M. Yan, Q. Jiang and X. B. Zhang, *Adv. Mater.*, 2017, **29**, 1604799.
2. C. Lv, Y. Qian, C. Yan, Y. Ding, Y. Liu, G. Chen and G. Yu, *Angew. Chem., Int. Ed.*, 2018, **57**, 10246-10250.
3. M. M. Shi, D. Bao, B. R. Wulan, Y. H. Li, Y. F. Zhang, J. M. Yan and Q. Jiang, *Adv. Mater.*, 2017, **29**, 1606550.
4. S.-J. Li, D. Bao, M.-M. Shi, B.-R. Wulan, J.-M. Yan and Q. Jiang, *Adv. Mater.*, 2017, **29**, 1700001.
5. R. Zhang, Y. Zhang, X. Ren, G. Cui, A. M. Asiri, B. Zheng and X. Sun, *ACS Sustainable Chem. Eng.*, 2018, **6**, 9545-9549.
6. J. Wang, L. Yu, L. Hu, G. Chen, H. Xin and X. Feng, *Nat. Commun.*, 2018, **9**, 1795.
7. H. Huang, L. Xia, X. Shi, A. M. Asiri and X. Sun, *Chem. Commun.*, 2018, **54**, 11427-11430.
8. J. Han, X. Ji, X. Ren, G. Cui, L. Li, F. Xie, H. Wang, B. Li and X. Sun, *J. Mater. Chem. A*, 2018, **6**, 12974-12977.
9. Z. Wang, C. Li, K. Deng, Y. Xu, H. Xue, X. Li, L. Wang and H. Wang, *ACS Sustainable Chem. Eng.*, 2018, **7**, 2400-2405.
10. Z. Wang, Y. Li, H. Yu, Y. Xu, H. Xue, X. Li, H. Wang and L. Wang, *ChemSusChem*, 2018, **11**, 3480-3485.
11. Y. Liu, Y. Su, X. Quan, X. Fan, S. Chen, H. Yu, H. Zhao, Y. Zhang and J. Zhao, *ACS Catal.*, 2018, **8**, 1186-1191.
12. S. Chen, S. Perathoner, C. Ampelli, C. Mebrahtu, D. Su and G. Centi, *Angew. Chem., Int. Ed.*, 2017, **56**, 2699-2703.